Two Dissociation Pathways of Water and Ammonia on the Si(001) Surface

Jung-Yup Lee and Jun-Hyung Cho*

Quantum Photonic Science Research Center, Hanyang University, 17 Haengdang-Dong, Seongdong-Ku, Seoul 133-791, Korea

Received: June 8, 2006

Using first-principles density-functional calculations, we investigated two competing pathways for the dissociation of water and ammonia on a Si(001) surface. For both systems, we found that, in addition to the conventionally accepted intradimer transfer of the H atom, the interdimer transfer of the H atom can be equally probable with the same reaction mechanism. Our analysis shows that the two dissociation pathways occur through the Lewis acid−base reaction between the partially positive H ion and the electron-abundant up atom of the buckled Si dimer. The result of the interdimer H transfer not only supports a recently proposed model for C-defect on Si(001) but also corresponds to the recent scanning tunneling microscopy data of ammonia dissociation on Si(001).

Introduction

Proton and H atom transfer phenomena are of fundamental importance in acid−base chemistry.[1,2] The simple but important example of the proton transfer may be the dissociation of water[3−5] (H_2O) and ammonia[6−13] (NH_3) molecules on the Si(001) surface. This dissociation is a key reaction in the chemical vapor deposition of silicon oxide and silicon nitride, which have become pervasive in the microelectronics industry. The Si(001) surface consists of rows of buckled dimers, where a partial charge transfer occurs from the down to the up Si atom,[14] therefore being partially positively and negatively charged, respectively. The initial interaction of H_2O (NH_3) with Si(001) occurs via a precursor in which the electron-deficient down Si atom attracts the lone pair of H_2O (NH_3) (see Figure 1).[5−12] As the next step, it is generally accepted that adsorbed H_2O (NH_3) dissociates into OH and H (NH_2 and H) species on the same dimer.[3−12] This dissociative arrangement is termed the on-dimer (OD) configuration. However, a recent scanning tunneling microscopy[13] (STM) experiment observed that there exists two distinct STM features for NH_3 dissociation on Si(001). One was assigned to the existing OD configuration, while the other was assigned to the inter-dimer (ID) configuration where the dissociated NH_2 and H are attached at the same side of two adjacent dimers along the dimer row. Thus, the conventional picture for the dissociation of H_2O (NH_3) on Si(001) is now being challenged.

There have been several theoretical and experimental studies for the intradimer and interdimer reactions of unsaturated hydrocarbons on the Si(001) surface. For the N−H dissociation of glycine on Si(001), Qu et al.[15] found that the formation of the ID configuration had a lower activation energy as compared to that of the OD configuration. Lu and Zhu[16] have shown that intradimer as well as interdimer reactions play an important role in the technologically important alkene/Si(001) chemistry. Using ab initio molecular dynamics calculations, Minary and Tuckerman[17] found that the reaction of butadiene on Si(001) yielded both the intradimer and the interdimer products, in good agreement with experimental observations.

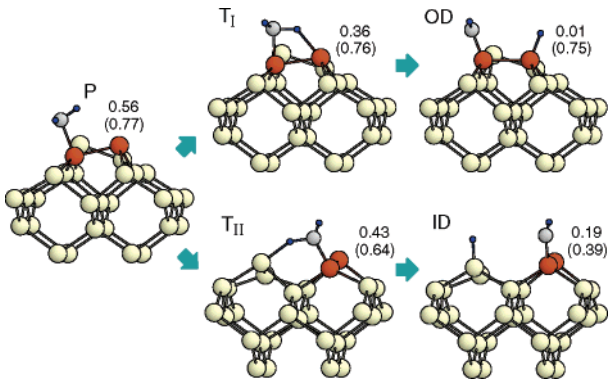

Figure 1. Atomic geometries of the precursor, transition, and dissociative states along path I (top) and path II (bottom)/H_2O dissociation on Si(001). The numbers denote the height difference (in angstroms) between the up and the down atoms of the reacted dimer (in red), while with those for the neighboring dimmer are in parentheses. The large, medium, and small circles represent Si, O, and H atoms, respectively.

In this paper, using first-principles density-functional theory[18] (DFT) calculations, we investigated the aforementioned two competing reactions in the dissociation of H_2O as well as NH_3 on Si(001). For the two systems, the energy barrier (E_b) from the precursor to the ID configuration was found to be slightly smaller than that from the precursor to the OD configuration, indicating that the formation of both configurations can be equally probable. The reaction pathway forming the OD (or ID) configuration is, hereafter, designated as path I (or path II). Our analysis shows that the dissociating H atom along each reaction pathway resembles a partially positive H ion rather than a bare proton. Hence, the OD and ID configurations are likely to be formed through the Lewis acid−base reaction between the partially positive H ion and the electron-abundant up atom. The formation of the ID configuration not only supports a recently proposed model[19] for C-defect on Si(001) whose origin and atomic structure have been one of the long-standing unsettled problems in surface science but also accords with the aforementioned STM data[13] of NH_3 dissociation on Si(001).

* Corresponding author. E-mail: chojh@hanyang.ac.kr.

10.1021/jp063564j CCC: $33.50
Published on Web 08/31/2006

TABLE 1: Calculated Adsorption Energies (in eV) of H_2O and NH_3 on Si(001), in Comparison with Previous Theoretical Results[a]

		P	T	D	E_b
H_2O	path I	0.64	0.39	2.35	0.25
		0.24−0.61[b]	0.08−0.49[b]	2.13−2.67[b]	0.04−0.30[b]
	path II	0.64	0.41	2.11	0.23
NH_3	path I	1.29	0.47	1.98	0.82
		1.13[c]		2.21[c]	
		0.94[d]		2.30[d]	
		1.21[e]		1.99[e]	
		1.31[f]		2.06[f]	
	path II	1.29	0.55	1.72	0.74
		1.31[f]		1.79[f]	

[a] P, T, and D denote the precursor, transition, and dissociative states, respectively. E_b denotes the energy barrier from the P to the T states. [b] From ref 5. [c] From ref 10. [d] From ref 11. [e] From ref 12. [f] From ref 13.

Calculations

We performed the total-energy and force calculations by using first-principles density-functional theory[18] within the generalized-gradient approximation (GGA). We used the exchange-correlation functional of Perdew et al.[20] for the GGA. The norm-conserving pseudopotentials of Si and H atoms were constructed by the scheme of Troullier and Martins[21] in the separable form of Kleinman and Bylander.[22] For N and O atoms whose 2s and 2p valence orbitals are strongly localized, we used the Vanderbilt ultrasoft pseudo-potentials.[23] The surface was modeled by the periodic slab geometry. Each slab contained six Si atomic layers, and the bottom Si layer was passivated by two H atoms per Si atom. The thickness of the vacuum region between these slabs is about 13 Å, and water and ammonia molecules were adsorbed on the unpassivated side of the slab. To make the interaction between adsorbed molecules sufficiently weak, we employed a 2×4 unit cell that involved four dimers along the dimer row. The electronic wave functions were expanded in a plane−wave basis set using a cutoff of 25 Ry, and the electron density was obtained from the wave functions at two k points in the surface Brillouin zone of the 2×4 unit cell. All the atoms except the bottom two Si layers were allowed to relax along the calculated Hellmann−Feynman forces until all the residual force components were less than 1 mRy/bohr.

Results

First, we determined the atomic structure of adsorbed H_2O on Si(001) within the precursor and dissociative configurations. The optimized structure for each configuration is shown in Figure 1. The calculated adsorption energies (E_{ads}) for various configurations are given in Table 1, together with previous[5] theoretical results. We find that the OD (E_{ads}= 2.35 eV) and ID (E_{ads}= 2.11 eV) configurations were significantly stabilized over the precursor state with E_{ads} = 0.64 eV. Our adsorption energies for the precursor and OD configurations were within the range of the corresponding values[5] obtained from a variety of cluster calculations using the Becke−Lee−Yang−Parr (BLYP) and B3LYP functionals[24] and the triple-ζ all-electron and Gaussian basis sets.

To examine the cleavage of the O−H bond, we calculated the energy profile for the dissociation by optimizing the structure with increasing the bond length d_{O-H}. Here, we optimized the structure by using the gradient projection method[25] where only the distance (but not the angles) between the O atom and the dissociating H atom was constrained. Hellmann−Feynman forces aid in the relaxation of all the atomic positions as well as the O−H bond angles for each of several values of the O−H bond length. In this way, we find a pathway to the final state along which the energy is everywhere a minimum for fixed bond length. The atomic geometries of the precursor (P), transition (T), and dissociative states in paths I and II are displayed in Figure 1. We obtain E_b = 0.23 eV from P to ID, slightly smaller than E_b = 0.25 eV from P to OD. Thus, we can say that both the OD and the ID configurations are almost equally formed on the surface. The formation of the ID configuration provides an explanation for a recent STM observation[19] that the atomic structure of the C-defect on Si(001) was interpreted in terms of the ID configuration.

TABLE 2: Calculated Electron Charge ρ_{MT} within the MT Sphere[a] Centered at the Dissociating H Atom/H_2O Dissociation on Si(001)

		P	T	D
H_2O	Path I	0.49	0.34	0.43
	Path II	0.49	0.34	0.42
NH_3[b]	Path I	0.50	0.33	0.43
	Path II	0.50	0.34	0.41

[a] Radius chosen to be 0.5 Å. [b] The results for NH_3 on Si(001) are also given.

Figure 1 shows that the height difference Δd_{up-dn} between the up and the down Si atoms varies during the H dissociation. Along path I, Δd_{up-dn} of the reacted dimer decreased to be almost zero at the OD configuration, while showing little change in the neighboring dimer. However, along path II, two adjacent dimers involved in the reaction show a large decrease of Δd_{up-dn} on going from P to ID. Considering the fact that buckling of the Si dimer accompanies charge transfer,[14] it is likely that in path I the charge redistribution occurred mostly at one reacted dimer, whereas in path II, it occurred across two adjacent dimers. We note that the up atom (bonding to the dissociating H atom) at T_{II} might be more negatively charged than that at T_I because of its increased buckling. Thus, the former up atom can more easily abstract a proton (or a partially positive H ion) from adsorbed H_2O through the Lewis acid−base reaction, resulting in a relatively lower energy barrier.

It is interesting to identify the charge character of the dissociating H atom whether it is a proton or a partially positive H ion. For this, we calculate the local charge ρ_{MT} inside the muffin-tin (MT) sphere centered at the dissociating H atom along the reaction pathways. The results are given in Table 2. We find that the changes of ρ_{MT} along paths I and II are almost the same as each other. The smallest magnitude of ρ_{MT} lies at the transition state. As shown in Table 2, ρ_{MT} at the transition state is reduced by ~31 (21)% as compared to that at the precursor (dissociative) state. This result leads us to conclude that the dissociating H atom would be a partially positive H ion rather than a bare proton. The corresponding local density of states (LDOS) at the dissociating H atom are displayed in Figure 2. We find the two peaks (located at −23.2 and −10.8 eV) at the precursor state, which are associated with O 2s and H 1s orbitals of the free H_2O molecule. These two peaks are significantly reduced at the T_I and T_{II} states (see Figure 2b,c, respectively), while the H 1s state hybridizes with the bands of the Si substrate, yielding a broadening of the LDOS. Such a broadening is enhanced at the OD and ID configurations. On the basis of the results of ρ_{MT} and the LDOS, we can say that the dissociating H atom shows a nearly identical charge character along paths I and II.

Parallel to the study of H_2O dissociation on Si(001), we calculated the energy profile for the N−H bond cleavage of NH_3. The atomic geometries of the precursor, transition, and

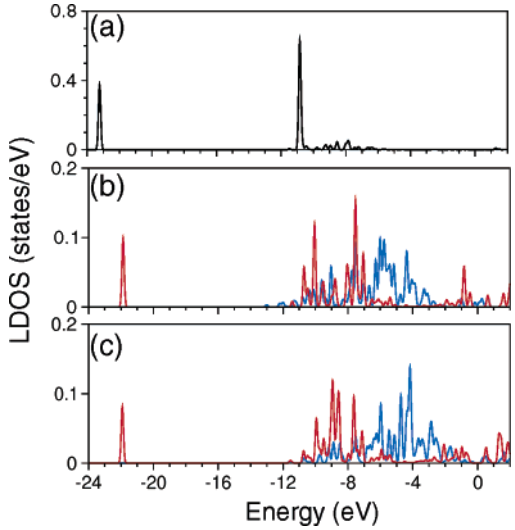

Figure 2. Calculated local density of states of ρ_{MT} (given in Table 2) for H_2O on Si(001): (a) the precursor, (b) T_I (red) and OD (blue), and (c) T_{II} (red) and ID (blue) states. The energy zero corresponds to the top of the valence band of each state.

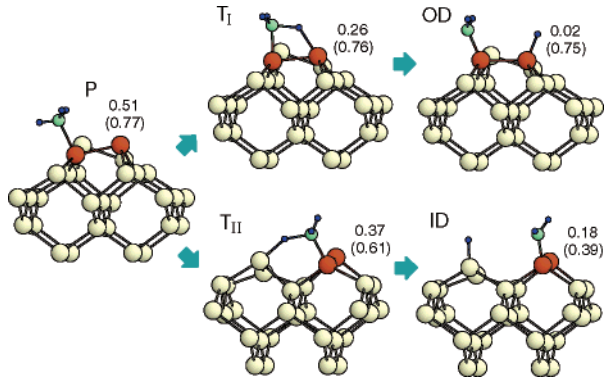

Figure 3. Atomic geometries of the precursor, transition, and dissociative states along path I (top) and path II (bottom)/NH_3 dissociation on Si(001). The numbers denote the height difference (in angstroms) between the up and the down atoms of the reacted dimer (in red), while those for the neighboring dimer are in parentheses. The large, medium, and small circles represent Si, N, and H atoms, respectively.

dissociative states in paths I and II are displayed in Figure 3, and their calculated adsorption energies are given in Table 1. As shown in Table 1, our calculated adsorption energies of various states agree well with previous[10−13] theoretical results. Similar to the case of H_2O, the OD configuration with E_{ads}= 1.98 eV is more stable than the ID configuration with E_{ads}= 1.72 eV, whereas E_b = 0.74 eV for the formation of the latter configuration is smaller than E_b = 0.82 eV for the formation of the former one. As shown in Figure 3, the trend of the decrease of the height difference Δd_{up-dn} between the up and the down Si atoms during the H dissociation is also similar to the case of H_2O. The calculated ρ_{MT} values within the muffin-tin (MT) sphere centered at the dissociating H atom along the reaction pathways are listed in Table 2, while the corresponding LDOS are displayed in Figure 4. We find that at the precursor state, the two peaks associated with N 2s and H 1s orbitals located at −20.0 and −10.0 eV, respectively (see Figure 4a). These are placed in a lower binding energy as compared to the O 2s and H 1s originating peaks (located at −23.2 and −10.8 eV, respectively) in the case of H_2O. However, the reduction of these two peaks at the T_I and T_{II} states as well as the broadening of the LDOS at the ID and OD configurations is similar to the case of H_2O.

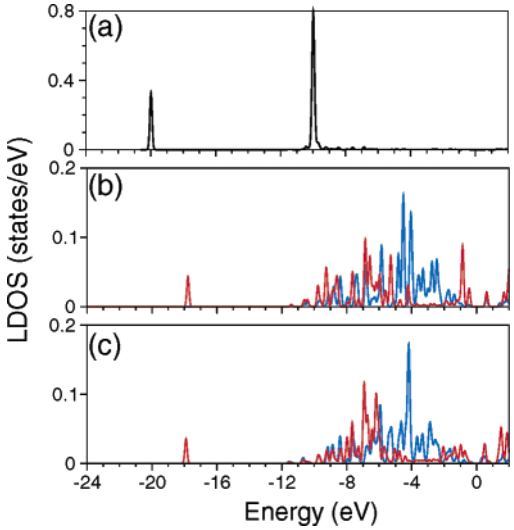

Figure 4. Calculated local density of states of ρ_{MT} (given in Table 2) for NH_3 on Si(001): (a) the precursor, (b) T_I (red) and OD (blue), and (c) T_{II} (red) and ID (blue) states. The energy zero corresponds to the top of the valence band of each state.

Thus, the general features for NH_3 dissociation on Si(001) are similar to those of the H_2O case, although the relative stabilities among the precursor, transition, and dissociative states differ from each other (see Table 1). Since the values of E_b for NH_3 dissociation are much larger than those for H_2O dissociation, adsorbed NH_3 may be somewhat trapped at the precursor, as observed in previous experiments.[9,26] Our calculated energy profile for NH_3 dissociation indicates that path II with E_b = 0.74 eV is kinetically favored over path I with E_b = 0.82 eV. Using an Arrhenius-type analysis, we estimate that at room temperature, the reaction rate from the P state to the ID configuration is ∼22 times larger than that from the P state to the OD configuration. However, this factor becomes 1.1 if all the adsorption energy of the precursor state is not dissipated during the reaction. These ratios should be reduced if one considers the effect of the flip−flop motion[27] of Si dimers at room temperature. We note that, if the down Si atoms of neighboring dimers are placed on the same side of adsorbed NH_3, the N−H dissociation along path II will be hindered by some repulsion between the partially positive H ion and the electron-deficient down atom. This may account for recent room-temperature STM data[13] showing that the population of the ID configuration is slightly smaller than that of the OD configuration.

Conclusion

Our calculations have shown that the dissociation of water and ammonia on Si(001) occurs via two facile reaction pathways. This can be generally applicable to various molecules containing hydroxyl and amino groups. Noting that the adsorption of those molecules on Si(001) was previously interpreted under the assumption that the H dissociation occurs on the same dimer,[28] we suggest that such a previous interpretation[8,29] could be reexamined, keeping in mind that interdimer dissociation could occur.

Acknowledgment. This work was supported by grant No. R01-2006-000-10920-0 from the Basic Research Program of the Korea Science and Engineering Foundation and by the MOST/KOSEF through the Quantum Photonic Science Research Center.

References and Notes

(1) Marx, D.; Tuckerman, M. E.; Hutter, J.; Parrinello, M. *Nature* **1999**, *397*, 601.
(2) Lu, D.; Voth, G. A. *J. Am. Chem. Soc.* **1998**, *120*, 4006.
(3) Chander, M.; Li, Y. Z.; Patrin, J. C.; Weaver, J. H. *Phys. Rev. B* **1992**, *48*, 2493.
(4) Raghavachari, K.; Chabal, Y. J.; Struck, L. M. *Chem. Phys. Lett.* **1996**, *252*, 230.
(5) Konecny, R.; Doren, D. J. *J. Chem. Phys.* **1997**, *106*, 2426.
(6) Queeney, K. T.; Chabal, Y. J.; Raghavachari, K. *Phys. Rev. Lett.* **2001**, *86*, 1046.
(7) Mui, C.; Wang, G. T.; Bent, S. F.; Musgrave, C. B. *J. Chem. Phys.* **2001**, *114*, 10170.
(8) Mui, C.; Han, J. H.; Wang, G. T.; Musgrave, C. B.; Bent, S. F. *J. Am. Chem. Soc.* **2002**, *124*, 4027.
(9) Hossain, M. Z.; Yamashita, Y.; Mukai, K.; Yoshinobu, J. *Phys. Rev. B* **2003**, *68*, 235322.
(10) Widjaja, Y.; Musgrave, C. B. *Phys. Rev. B* **2001**, *64*, 205303.
(11) Xu, X.; Kang, S. Y.; Yamabe, T. *Phys. Rev. Lett.* **2002**, *88*, 076106.
(12) Lee, S. H.; Kang, M. H. *Phys. Rev. B* **1998**, *58*, 4903.
(13) Chung, O. N.; Kim, H.; Chung, S.; Koo, J. *Phys. Rev. B* **2006**, *73*, 033303.
(14) Chadi, D. J. *Phys. Rev. Lett.* **1979**, *43*, 43.
(15) Qu, Y. Q.; Wang, Y.; Li, J.; Han, K. L. *Surf. Sci.* **2004**, *569*, 12.
(16) Lu, X.; Zhu, M. *Chem. Phys. Lett.* **2004**, *393*, 124.
(17) Minary, P.; Tuckerman, M. E. *J. Am. Chem. Soc.* **2005**, *127*, 1110.
(18) Hohenberg, P.; Kohn, W. *Phys. Rev.* **1964**, *136*, B864. Kohn, W.; Sham, L. J. *Phys. Rev.* **1965**, *140*, A1133.
(19) Hossain, M. Z.; Yamashita, Y.; Mukai, K.; Yoshinobu, J. *Phys. Rev. B* **2003**, *67*, 153307.
(20) Perdew, J. P.; Burke, K.; Ernzerhof, M. *Phys. Rev. Lett.* **1996**, *77*, 3865.
(21) Troullier, N.; Martins, J. L. *Phys. Rev. B* **1991**, *43*, 1993.
(22) Kleinman, L.; Bylander, D. M. *Phys. Rev. Lett.* **1982**, *48*, 1425.
(23) Vanderbilt, D. *Phys. Rev. B* **1990**, *41*, 7892. Laasonen, K.; Pasquarello, A.; Car, R.; Lee, C.; Vanderbilt, D. *Phys. Rev. B* **1993**, *47*, 10142.
(24) Becke, A. D. *Phys. Rev. A* **1998**, 38, 3098. Lee, C.; Yang, W.; Parr, R. G. *Phys. Rev. B* **1998**, *37*, 785. Becke, A. D. *J. Chem. Phys.* **1993**, *98*, 5648.
(25) Wismer, D. A.; Chattery, R. *Introduction to Nonlinear Optimization*; North-Holland: Amsterdam, 1978; pp 174−178.
(26) Takaoka, T.; Kusunoki, I. *Surf. Sci.* **1998**, *412*−*413*, 30.
(27) Dabrowski, J.; Scheffler, M. *Appl. Surf. Sci.* **1992**, *56*, 15.
(28) Lu, X.; Zhang, Q.; Lin, M. C. *Phys. Chem. Chem. Phys.* **2001**, *3*, 2156.
(29) Shannon, C.; Campion, A. *Surf. Sci.* **1990**, *227*, 219.